ROJ Radiation Oncology Journal

Original Article

pISSN 2234-1900 · eISSN 2234-3156
Radiat Oncol J 2026;44(1):69-78
https://doi.org/10.3857/roj.2025.00619

Morphological variation in rectal hydrogel spacer one month after insertion during low-dose-rate brachytherapy for prostate adenocarcinoma

Hyeok Choi[1], Seo Jin Lee[1], Yeonok Park[1,2], Wooshik Kim[1], Ho Lee[1], Jaeho Cho[1]

[1]*Department of Radiation Oncology, Yonsei Cancer Center, Heavy Ion Therapy Research Institute, Yonsei University College of Medicine, Seoul, Republic of Korea*
[2]*Proton Therapy Center, National Cancer Center, Goyang, Republic of Korea*

Received: September 18, 2025
Revised: January 8, 2026
Accepted: January 26, 2026

Correspondence:
Jaeho Cho
Department of Radiation Oncology, Yonsei Cancer Center, Heavy Ion Therapy Research Institute, Yonsei University College of Medicine, 50 Yonsei-ro, Seodaemun-gu, Seoul 03722, Republic of Korea
Tel: +82-2-2228-9095
E-mail: jjhmd@yuhs.ac
ORCID:
https://orcid.org/0000-0001-9966-5157

Purpose: This study aimed to develop and validate a 10-point, threshold-based variation score (VS) that integrates magnetic resonance imaging (MRI)–derived spacer morphology and assesses its association with rectal dose after low-dose-rate (LDR) prostate brachytherapy.

Materials and Methods: We retrospectively studied 149 men treated with iodine-125 LDR brachytherapy and polyethylene-glycol spacers (August 2022–April 2023). Using day 30 fused computed tomography–MRI, the VS assigned one point each for total volume >5 mL; hemisphere volumes (apex, base, left, and right) >5 mL; midgland thickness >5 mm; and thickness >5 mm 1-cm toward apex, base, left, and right. Univariable linear regression tested VS versus change in rectal D1cc (maximum dose to 1 mL). Bonferroni-adjusted Fisher's exact tests evaluated component differences across prespecified VS thresholds (≥6, ≥8, and 10).

Results: Median rectal D1cc decreased from 92.4% pre-spacer to 53.4% of prescription at day 30. Each one-point higher VS was associated with 5.4 Gy lower D1cc (95% confidence interval, 3.4 to 7.4; $p < 0.001$, $R^2 = 0.166$). Threshold analyses identified key contributors: midgland separation distinguished VS <6 from 6–7 (adequacy 57%→100%; adjusted $p = 0.026$); uniform directional thickness, especially apical, distinguished 6–7 from 8–9 (22%→91%; adjusted $p < 0.001$); apical volume >5 mL was required for VS = 10 (19%→100%; adjusted $p < 0.001$).

Conclusion: VS is a simple, objective metric linking spacer morphology with rectal dose reduction. Threshold-oriented targets, midgland separation for VS ≥ 6, uniform thickness for VS ≥ 8, and robust apical volume for VS = 10, may guide technical optimization and quality assurance in prostate LDR brachytherapy.

Keywords: Prostatic neoplasms, Brachytherapy, Hydrogels, Rectum

Introduction

Low-dose-rate (LDR) brachytherapy achieves durable biochemical control in low-risk prostate cancer [1], yet rectal irradiation remains a concern across prostate radiotherapy modalities. Perirectal hydrogel spacers reduce rectal dose by separating the rectum and prostate, with reported decreases in rectal D1cc (maximum dose to 1 mL) from 94.2% to 52.4% of prescription ($p < 0.001$) and lower gastrointestinal toxicity [2-4]. Nevertheless, follow-up imaging shows substantial variability in spacer morphology, raising questions about stability, reproducibility, and consistent clinical effect [5].

Post-insertion geometry has been assessed with computed tomography (CT)/magnetic resonance imaging (MRI) using regional

thickness, base-midgland-apex measurements, and geometric indices of asymmetry [6-8]. Although mild asymmetry may still outperform no spacer [9], existing methods do not provide a standardized, objective metric that integrates multiple morphological parameters for routine evaluation.

At our institution, spacer placement immediately after iodine-125 seed implantation became standard in August 2022. To address morphological variation, we developed a 10-point variation score (VS) that consolidates volume and thickness features from day 30 CT/MRI into a single measure. This study evaluates the VS-rectal dosimetry association and identifies morphology thresholds to guide post-procedural quality assurance.

Materials and Methods

1. Patient selection

We retrospectively reviewed 149 consecutive patients with clinically localized prostate adenocarcinoma who underwent LDR brachytherapy with rectal hydrogel spacer placement between August 1, 2022, and April 30, 2023. Disease risk ranged from low to organ-confined high risk. We collected baseline clinicopathologic variables, including biopsy Gleason grade, prostate-specific antigen (PSA), multiparametric MRI findings, and androgen-deprivation therapy from initial consultation through the 1-month follow-up. Spacer use was routinely offered and ultimately determined by patient preference.

2. Simulation, procedure, and dosimetry analysis

Pre-implant planning followed standard transrectal ultrasound (TRUS) workflows. Organs at risk (rectum and urethra) and the prostate were contoured, and a prescription of 145 Gy to the planning target volume was used. Iodine-125 seeds were implanted with real-time intraoperative planning. Hydrogel spacer placement was performed immediately afterward in the same session. Dosimetry was evaluated at three time points: pre-spacer, day 0, and day 30 (Fig. 1). We recorded prostate coverage (D90% [dose to 90% of the structure volume], V100% [100% of the prescribed dose], V150% [150% of the prescribed dose], and V200% [200% of the prescribed dose]), urethral V200 Gy (mL), and rectal V100% (mL).

Spacer insertion used standard TRUS guidance. The needle was advanced into the perirectal space. Saline hydrodissection was performed using the necessary amount from a prepared 10-mL syringe. The hydrogel (10-mL polyethylene-glycol, SpaceOAR, Boston Scientific, Marlborough, MA, USA) was then injected slowly to achieve uniform posterior coverage from base to apex. A non-contrast CT was obtained on day 0. At day 30, a T2-weighted MRI was fused with same-day non-contrast CT. Rectum and spacer were re-contoured on MRI, prostate contours were transferred, and seed positions were verified on CT to ensure dosimetric accuracy and allow assessment of spacer stability and anatomic relationships. Spacer volume on MRI was defined as the T2-hyperintense compartment between the rectum and prostate, encompassing the hydrogel and surrounding fluid signal, rather than the injected material volume alone.

3. Morphological evaluation of spacer

Day 30 CT-MRI served as the morphology reference (Fig. 2). Orthogonal planes through the prostate centroid partitioned the

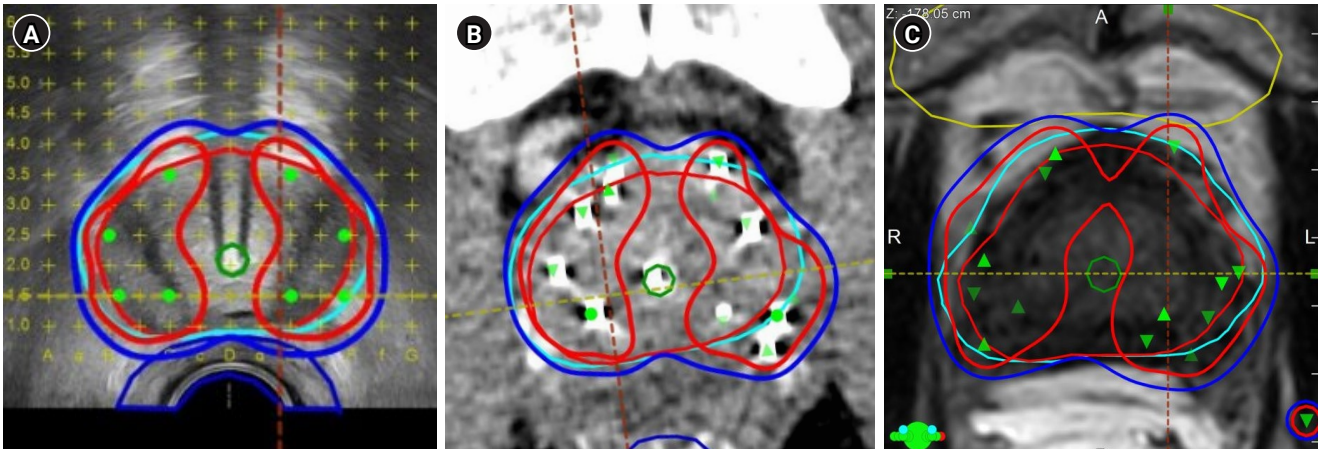

Fig. 1. Imaging modalities at different stages of low-dose-rate brachytherapy with hydrogel spacer insertion. (A) Transrectal ultrasound obtained during treatment planning, with the same modality used for intraoperative 4D adaptive planning and pre-spacer evaluation. (B) Computed tomography performed on day 0. (C) T2-weighted magnetic resonance imaging acquired on day 30 for follow-up assessment. Thin red line: prostate; thin sky-blue line: PTV; thick red line: 150% isodose; thick blue line: 100% isodose; green line: ureter; yellow line: bladder; green dots: seed positions.

https://doi.org/10.3857/roj.2025.00619

Fig. 2. Magnetic resonance imaging (MRI)–based spacer measurements relative to the prostate midgland. Sagittal and axial T2-weighted MRIs showing spacer thickness at the prostate midgland and at 1 cm in four directions (apex, base, left, and right), along with hemisphere volumes segmented by axial and sagittal planes through the midgland.

spacer into apex, base, left, and right hemivolumes. Thickness was measured at the midgland and at 1-cm offsets toward the apex, base, left, and right, defined as the shortest prostate-rectum separation at each location. Volumes and thicknesses were derived from MIM Maestro v7.2 contours; RT-structure DICOM files were exported and processed in MATLAB R2025a.

To summarize morphology for routine use, we devised a 10-point VS comprising five volumetric and five thickness components. One point was awarded for total spacer volume >5 mL; one each for hemivolumes (apex, base, left, and right) >5 mL; one for midgland thickness >5 mm; and one each for directional thickness >5 mm at 1-cm offsets toward apex, base, left, and right. Thresholds (5 mm, 5 mL) were chosen for procedural simplicity (TRUS 5-mm grid; 10-mL syringe). The VS thus yields a single integer (0–10) reflecting overall spacer adequacy suitable for post-procedure quality assurance.

4. Statistical analysis

The primary endpoint was change in rectal D1cc from pre-spacer to day 30 (ΔD1cc). The main analysis assessed the association between VS (treated as an ordinal variable) and ΔD1cc using univariable linear regression. We report slope estimates (Gy per VS point), 95% confidence intervals (CIs), p-values, and goodness-of-fit metrics. Model assumptions were checked graphically (linearity, homoscedasticity, and influential observations). Because volume and thickness components may co-vary, we explored potential multicollinearity descriptively.

Patients were stratified into prespecified VS groups (<6, 6–7, 8–9, and 10) to examine stepwise adequacy of individual components. For each component, we computed the proportion of patients meeting the criterion within each VS group. To identify features that differentiate successive groups, we compared adjacent strata (VS < 6 vs. 6–7, 6–7 vs. 8–9, and 8–9 vs. 10). In addition, because clinical decision-making often uses score thresholds, we evaluated two thresholds a priori (VS ≥ 6 and VS ≥ 8) and the maximum (VS = 10) to highlight morphology targets that correspond to progressively higher overall VS. Fisher exact tests were used for categorical contrasts with Bonferroni adjustment for the set of pairwise comparisons within each component; adjusted $p < 0.05$ was considered statistically significant.

Results

1. Patient characteristics

We reviewed the medical records of 149 patients who underwent LDR brachytherapy with hydrogel spacer insertion between August 1, 2022, and April 30, 2023. The median patient age was 68 years, and the median pre-treatment PSA level was 6.97 ng/mL. Gleason scores were 5 (3 + 2) in one patient, 6 (3 + 3) in 53 patients, 7 (3 + 4) in 38, 7 (4 + 3) in 25, and ≥8 in 32. Clinical T stage was most commonly T2a (n = 72), with the remainder classified as T1c or T2b–T2c. Androgen deprivation therapy was administered to 80 patients, primarily those with high-risk disease in accordance with National Comprehensive Cancer Network guidelines. The mean prostate volume was 30 mL, and treatment plans typically included a median of 76 iodine-125 seeds delivered via a median of 20 needles per patient.

2. Dosimetry evaluation

Prostate and urethral dosimetry parameters were evaluated at three time points (pre-spacer, day 0, and day 30) to confirm procedural safety (Table 1). Hydrogel spacer insertion did not compromise planning objectives for either the prostate or urethra. All patients (n = 149, 100%) consistently achieved the prostate D90% goal of > 145 Gy, with prostate V100% remaining stable at 97.5% pre-spacer, 97.3% on day 0, and 97.0% on day 30. Urethral V200Gy was 0 mL in 99% of patients on pre-spacer, 100% on day 0, and 99% on day 30, meeting urethral dose constraints throughout. In contrast, rectal dosimetry improved substantially following spacer insertion. While only 79% of patients satisfied the rectal V145 Gy < 1 mL constraint pre-spacer, 100% met this criterion by day 30. This outcome reflected both the spacer's efficacy and a planning strategy that anticipated post-insertion rectal dose reduction.

Table 1. Prostate coverage and dose constraint fulfillment demonstrating dosimetric stability following spacer insertion

	Pre-spacer	Day 0	Day 30
Prostate D90% > 145 Gy	149 (100)	149 (100)	149 (100)
Urethra V200 Gy = 0 mL	147 (98.7)	149 (100)	147 (98.7)
Prostate V100% (%)	97.5 ± 1.6	97.3 ± 1.4	97.0 ± 1.7
Prostate V150% (%)	49.4 ± 5.3	49.3 ± 5.7	55.0 ± 7.4
Prostate V200% (%)	16.9 ± 3.9	16.3 ± 4.5	22.7 ± 6.3

Values are presented as number (%) or mean ± standard deviation.
Prostate and urethral dosimetry parameters are shown at pre-spacer, day 0, and day 30 to confirm that hydrogel spacer insertion did not adversely affect target coverage or urethral dose constraints.
D90%, dose to 90% of the structure volume; V100%, 100% of the prescribed dose; V150%, 150% of the prescribed dose; V200%, 200% of the prescribed dose.

Rectal dose-volume histogram (DVH) analysis demonstrated a marked reduction in rectal dose from pre-spacer to day 30 (Fig. 3). Median DVH curves were calculated from patient-level data, with interquartile ranges (IQRs) shown as envelopes. The pre-spacer median DVH is shown in black with a gray envelope; the day 30 DVH is shown in red with a pink envelope. The median rectal D1cc decreased from 92.4% (IQR, 88.6 to 94.9%) of the 145 Gy prescription to 53.4% (IQR, 44.4 to 63.3%) on day 30. Additionally, the low-dose volume was reduced across the curve, with no overlap between the IQR envelopes, underscoring the spacer's effectiveness in lowering rectal dose.

3. Morphological variation

Spacer morphology was evaluated in terms of volume and thick-

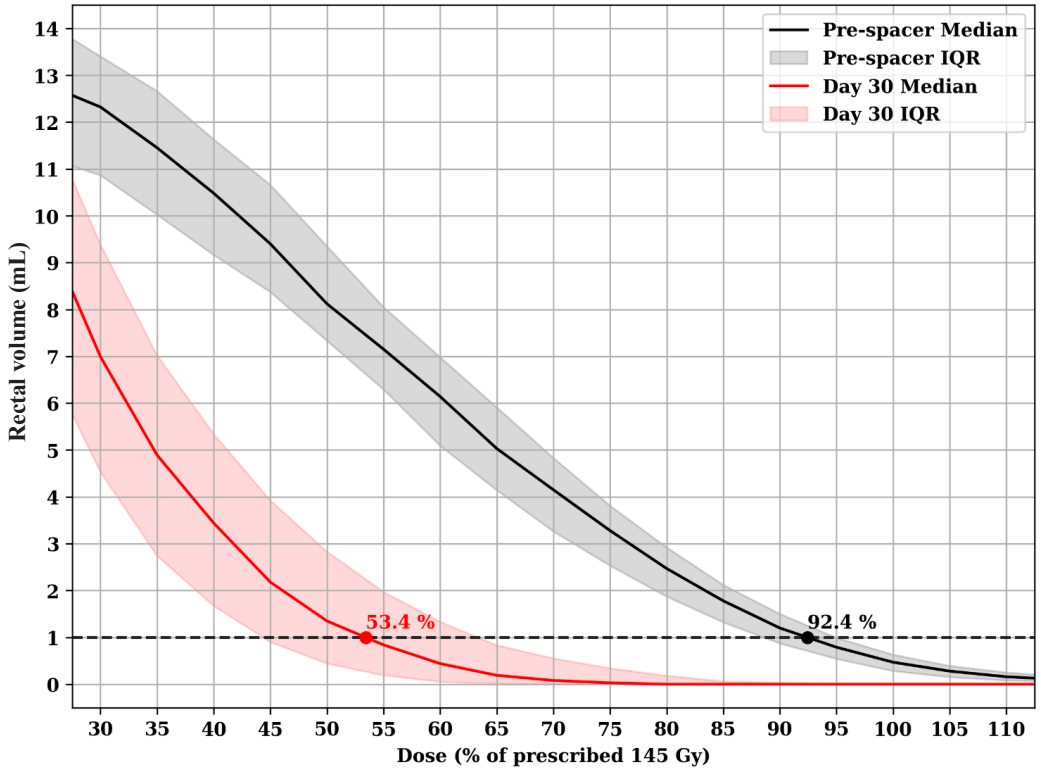

Fig. 3. Rectal dose-volume histograms pre-spacer and day 30. Rectal D1cc (maximum dose to 1 mL) decreased from 92.4% (interquartile range [IQR], 88.6% to 94.9%) pre-spacer to 53.4% (IQR, 44.4% to 63.3%) on day 30 of the 145 Gy prescription, demonstrating substantial rectal dose reduction.

https://doi.org/10.3857/roj.2025.00619

ness in four cardinal directions (apex, base, left, and right) (Fig. 4A). Total spacer volume was generally consistent across patients, with a median of 15.5 mL (IQR, 14.4 to 16.9). Hemivolume analysis revealed asymmetry: apex hemisphere was markedly smaller at 4.6 mL (IQR, 2.6 to 6.6), while the base hemisphere had a median volume of 10.9 mL (IQR, 8.0 to 13.1). Left and right volumes were more symmetric, with medians of 6.9 mL (IQR, 5.7 to 8.4) and 8.4 mL (IQR, 6.9 to 9.7), respectively. Spacer thickness at the prostate midgland measured 12.0 mm (IQR, 9.5 to 14.0). At 1-cm offsets, thickness declined: 11.0 mm (IQR, 7.0 to 13.0) apex, 12.0 mm (IQR, 10.0 to 14.0) base, and 10.0 mm laterally (IQR, 6.5 to 12.0 left, 7.0 to 13.0 right). Boxplots (Fig. 4B) highlighted apex-base asymmetry in both volume and thickness. Base regions consistently showed greater and more uniform expansion, while the apex region demonstrated reduced and more variable values. Left-right morphology remained relatively balanced. These findings indicate that although total spacer volume aligned with intended injection goals, directional variation, particularly apex, was significant and may influence rectal dosimetry.

Across 149 patients, VS ranged from 4 to 10 (median 9) and rose modestly with later cases, as reflected by a Spearman rank correlation ($\rho = 0.15$, $p = 0.075$), suggesting a procedural learning-curve trend (Fig. 5A). Apex thickness fell below the adequacy threshold in 30 patients (20%), and apex volume in 82 patients (55%). In contrast, total volume and lateral symmetry were consistently achieved. These results suggest that although overall spacer deployment was effective, achieving sufficient apex spread, both in thickness and volume, was more technically challenging, likely due to anatomical constraints and needle trajectory variation. Representative day 30 T2-weighted magnetic resonance images (Fig. 5B)

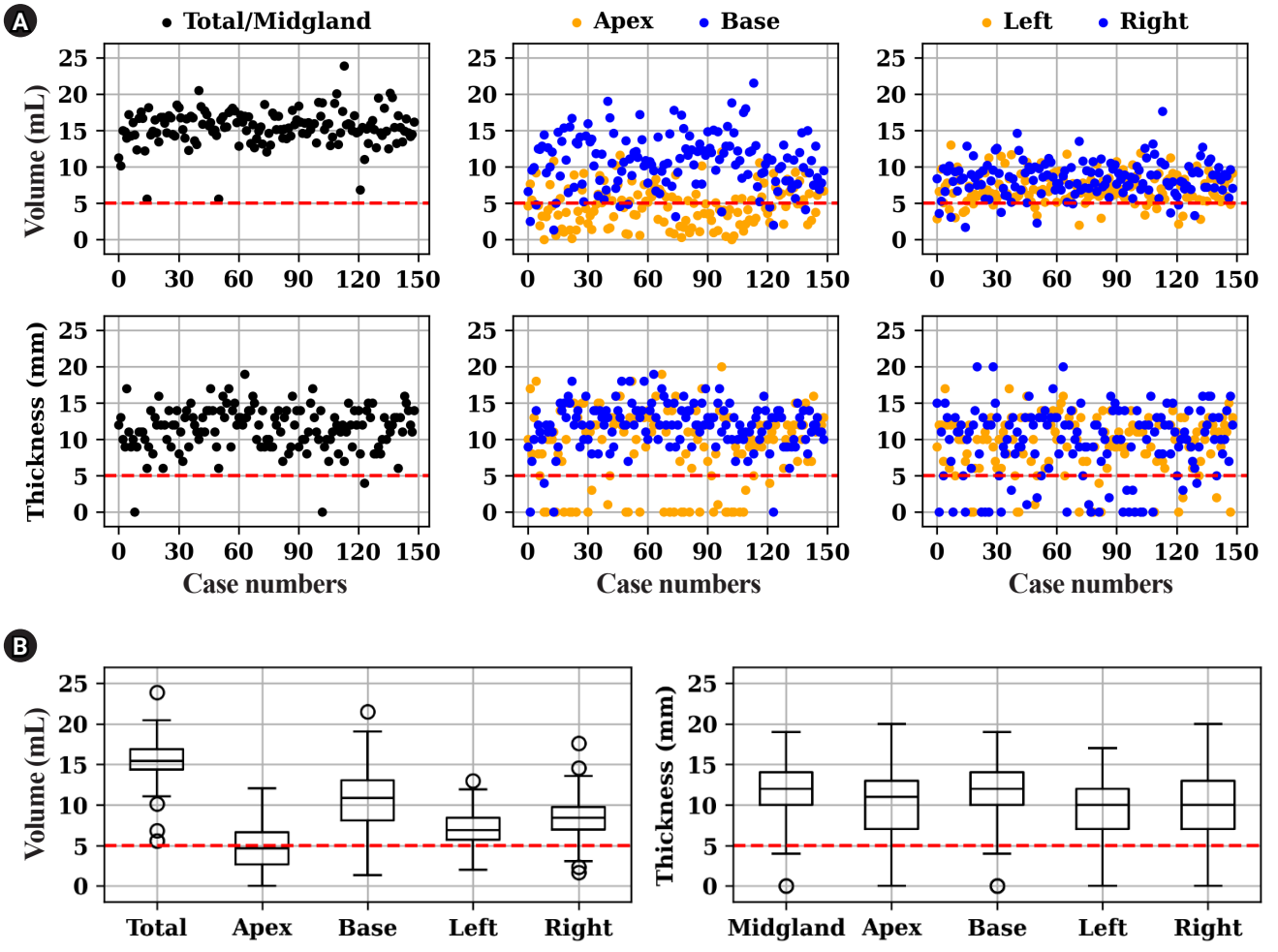

Fig. 4. Spacer volume and thickness distributions across cases. (A) Scatter plots showing total and hemisphere spacer volumes and thicknesses (apex, base, left, and right) by case. Red dashed lines mark thresholds: 5 mL for volume, 5 mm for thickness. (B) Boxplots of total and hemisphere volumes (in mL) and spacer thickness (in mm) at the midgland and at 1 cm intervals in four directions. Thresholds indicated by red dashed lines.

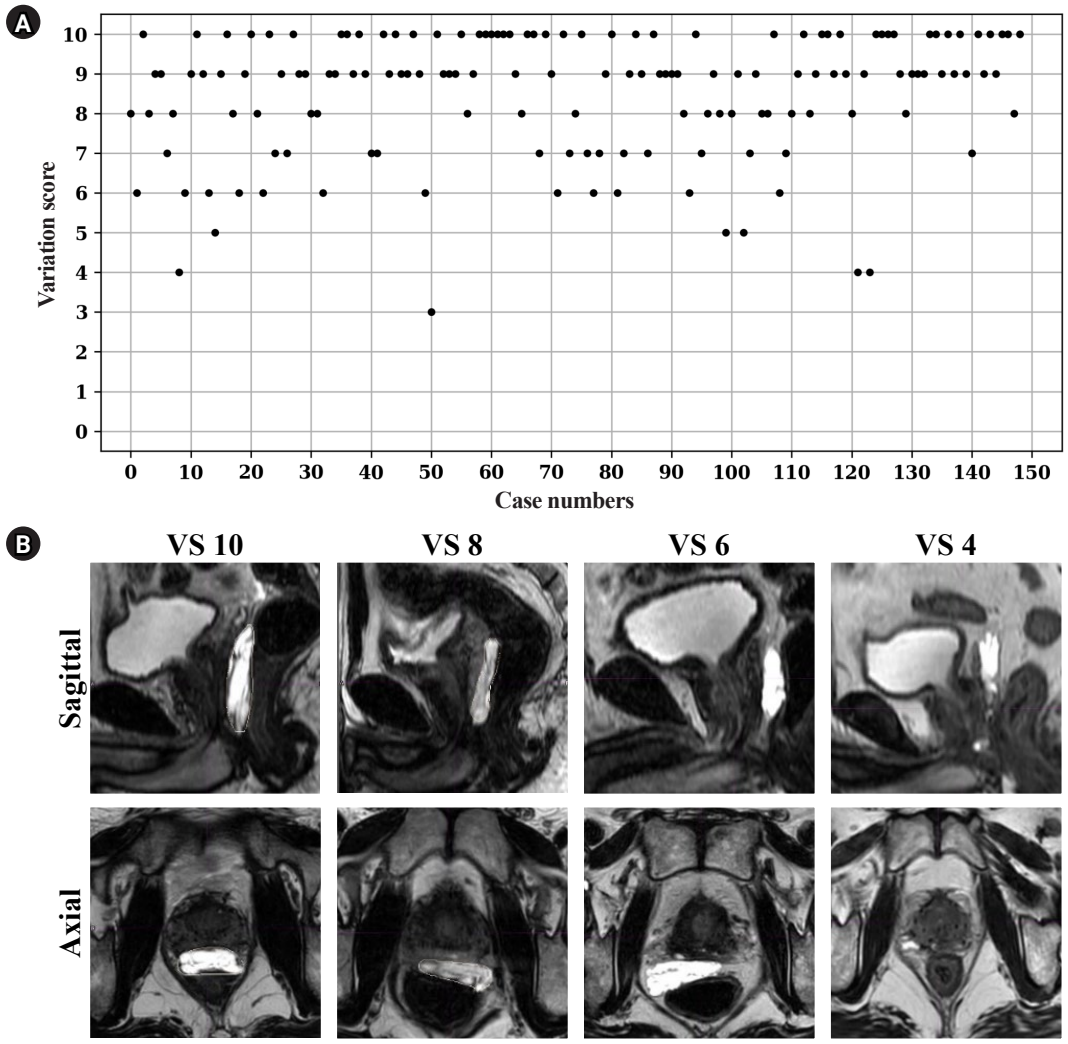

Fig. 5. Spacer variation scores and day 30 magnetic resonance imaging (MRI) morphology. (A) Scatter plot of variation scores (VS; max 10), with 1 point each for total volume >5 mL, hemisphere volumes (apex, base, left, and right) >5 mL, and thickness >5 mm at midgland and 1 cm in four directions. Most cases scored 8–10, indicating sufficient rectal spacing. (B) Day 30 T2-weighted MRIs from four patients (scores 10, 8, 6, and 4; top left to bottom right). Each shows sagittal and axial views. Higher scores show well-preserved spacer; lower scores show volume loss and irregularity.

illustrate spacer morphology across a range of VS (10, 8, 6, and 4). A score of 10 showed uniform, symmetric expansion and rectal separation in all directions. A score of 8 exhibited mild under-expansion, often in apex or lateral regions, but maintained acceptable overall morphology. A score of 6 revealed more pronounced deficiencies, especially apex thinning and asymmetry. The lowest-scoring case (score 4) showed collapsed morphology with minimal apex separation, likely due to suboptimal injection or early hydrogel absorption. These examples support the utility of the 10-point VS in identifying suboptimal spacer outcomes that may compromise dosimetric performance. Additionally, univariable linear regression indicated that each one-point increase in VS reduced rectal D1cc by 5.4 Gy from pre-spacer to day 30 (95% CI, 3.4 to 7.4 Gy; $p < 0.001$, $R^2 = 0.166$), a drop equivalent to 3.7% of the 145 Gy prescription dose.

Patients were stratified into four ascending VS subgroups, VS < 6 (n = 7), VS 6–7 (n = 23), VS 8–9 (n = 68), and VS 10 (n = 51), and each adequacy criterion was tested sequentially (Table 2). Moving beyond VS 6 hinged on satisfying the midgland thickness benchmark, adequacy rose from four patients (57.1%) in the VS < 6 subgroup to 23 patients (100%) at VS 6–7, Bonferroni-adjusted p = 0.026. Progressing past VS 8 depended on directional thickness, apex adequacy jumped from five patients (21.7%) at VS 6–7 to 62 patients (91.2%) at VS 8–9, while left and right thickness improved from nine patients (39.1%) and 10 patients (43.5%) to 64 patients (94.1%) and 62 patients (91.2%), respectively, all adjusted p <

 https://doi.org/10.3857/roj.2025.00619

Table 2. Variation-score adequacy and Bonferroni-adjusted Fisher p-values

Criterion	Variation-score group			p-value		
	< 6 (n = 7)	6–7 (n = 23)	8–9 (n = 68)	< 6 vs. 6–7	6–7 vs. 8–9	8–9 vs. 10
Volume ≥ 5 mL						
Total	7 (100)	23 (100)	68 (100)	1.000	1.000	1.000
Apex	1 (14.3)	2 (8.7)	13 (19.1)	1.000	1.000	< 0.001[a]
Base	4 (57.1)	21 (91.3)	63 (92.6)	0.204	1.000	0.210
Left	2 (28.6)	17 (73.9)	59 (86.8)	0.204	0.582	0.030[a]
Right	4 (57.1)	20 (87.0)	65 (95.6)	0.360	0.501	0.777
Thickness ≥ 5 mm						
Midgland	4 (57.1)	23 (100)	68 (100)	0.026[a]	1.000	1.000
Apex	1 (14.3)	5 (21.7)	62 (91.2)	1.000	< 0.001[a]	0.110
Base	5 (71.4)	21 (91.3)	68 (100)	0.674	0.185	1.000
Left	2 (28.6)	9 (39.1)	64 (94.1)	1.000	< 0.001[a]	0.402
Right	1 (14.3)	10 (43.5)	62 (91.2)	0.644	< 0.001[a]	0.110

Values are presented as number (%).
Each cell shows pass counts and percentage within the subgroup. p-values are from two-sided Fisher exact tests, Bonferroni-adjusted for the three pairwise comparisons.
[a]Bonferroni-adjusted two-sided Fisher exact $p < 0.05$.

0.001. Attaining VS 10 required an additional volumetric milestone, apical volume adequacy climbed from 13 patients (19.1%) in VS 8–9 to 51 patients (100%) in VS 10 (adjusted $p < 0.001$), and left-hemisphere volume rose from 59 patients (86.8%) to 51 patients (100%) ($p = 0.030$).

Discussion and Conclusion

Rectal hydrogel spacers have become an indispensable adjunct in prostate radiotherapy; however, the quality of spacer deployment remains highly operator dependent. In this study of patients undergoing LDR brachytherapy, we demonstrate that spacer morphology, rather than spacer presence alone, plays a critical role in determining rectal dose reduction while preserving prostate dosimetry. To objectively capture this geometric variability, we introduce a novel 10-point VS that integrates regional volume and thickness thresholds. This framework provides a practical, morphology-based approach for quality assessment and offers new insight into geometry–dose relationships in spacer-assisted brachytherapy.

Several technical innovations reported in external-beam radiotherapy cohorts align conceptually with our findings. Prior studies have shown that CT-based pre- and post-procedural distance mapping can identify suboptimal separations earlier than delayed MRI assessment, while probe-mounted, TRUS-guided needle systems improve trajectory control and spacer symmetry [10,11]. Apex-first injection techniques, which we adopted in this series, have been associated with improved caudal separation and reduced apex rectal dose compared with conventional midgland delivery [12]. The recent development of radiopaque spacers enables real-time verification using cone-beam CT, potentially obviating the need for post-procedural MRI [13,14]. Additional strategies, including faster-setting polyethylene-glycol formulations and dual-track injection techniques, have been proposed to enhance longitudinal continuity in anatomically narrow Denonvilliers' fascia [15]. Balloon-type biodegradable spacers represent another approach to shape stability, although clinical experience remains limited [16].

Because the hydrogel spacer is radiolucent on CT, direct assessment of spacer morphology was not feasible using post-implant CT alone, necessitating MRI follow-up. Day 30 imaging is particularly relevant in LDR brachytherapy, as a substantial proportion of the iodine-125 dose is delivered within the first 3 months, making early spacer configuration representative of the period during which most dose is deposited.

In this context, it is important to emphasize that the VS was designed as a cross-sectional descriptor of post-procedural spacer morphology, rather than a metric intended to capture temporal variability or longitudinal stability. Although the VS is derived from day 30 imaging alone, this time point remains clinically meaningful in LDR brachytherapy, because the majority of rectal dose deposition occurs during the early post-implant period. Accordingly, the spacer configuration observed at 1 month is representative of the geometric conditions during the period of highest rectal dose exposure. Within this framework, the VS consolidates multidimensional geometric characteristics into a single operational indicator that permits straightforward comparison across patients and operators and can function as a procedural quality descriptor alongside

conventional dose metrics.

The nominal hydrogel material volume was 10 mL, whereas the median day 30 MRI-derived volume was 15.5 mL. This difference is attributable to early water uptake by the polyethylene-glycol material, including incorporation of residual saline from hydrodissection, as well as inclusion of perihydrogel T2-hyperintense edema and interpolation effects from CT-MRI fusion. Prior MRI-based studies have demonstrated that the apparent volume of polyethylene-glycol hydrogel spacers may increase after placement due to intrinsic material properties. In a quantitative MRI study using Dixon-based water-only imaging, Hama and Tate [17] reported that the volume of SpaceOAR increased by up to approximately 20% during the weeks following implantation, reflecting early water uptake rather than true overfilling or measurement error. In the present study, the median MRI-derived spacer volume at 1 month exceeded the nominal injected volume beyond this range in a subset of patients. This discrepancy can be explained by the nature of T2-weighted MRI–based segmentation, which delineates the entire hyperintense compartment between the rectum and prostate rather than the injected hydrogel material alone. This compartment may include pre-existing perirectal space along the Denonvilliers' fascia, residual saline from hydrodissection, perihydrogel edema, and partial volume effects from CT-MRI fusion. Accordingly, MRI-derived spacer volume should be interpreted as an apparent rectoprostatic separation compartment rather than a direct measure of the injected hydrogel volume.

Within this framework, the VS showed a statistically significant association with rectal dose reduction (ΔD1cc), although the model explained only a limited proportion of variability (R^2 = 0.166). To further illustrate this relationship, a scatter plot of VS versus ΔD1cc with the fitted regression line is provided in Supplementary Fig. S1, demonstrating the overall directionality and dispersion of the data. This modest explanatory power likely reflects the multifactorial nature of rectal dose geometry in LDR brachytherapy, where baseline rectal anatomy, seed distribution, prostate deformation, and implantation technique may all contribute to inter-patient variability. Importantly, this finding does not diminish the utility of the VS but rather underscores its role as a practical quality indicator within a complex dosimetric environment. Rather than replacing dosimetric evaluation, the VS is intended to complement CT-based dose metrics by providing a standardized geometric quality indicator that facilitates post-procedural quality assurance, inter-operator comparison, and assessment of technical adequacy in spacer deployment. Importantly, the VS was not developed as an outcome or toxicity prediction metric, but as a procedural quality assessment tool that characterizes spacer geometry beyond what can be inferred from rectal dose metrics alone. Accordingly, the VS should be interpreted strictly as a procedural quality metric rather than a surrogate for clinical outcome or toxicity.

The rationale for incorporating both thickness and volume components into the VS is that these parameters capture complementary and non-substitutable aspects of spacer geometry. Thickness measurements reflect focal minimal rectoprostatic separation at specific anatomic locations, whereas hemispheric volume characterizes longitudinal continuity and directional distribution of the spacer along the rectoprostatic interface—features that cannot be inferred from point-based thickness measurements alone. Accordingly, the composite VS was designed to summarize multiple dimensions of deployment quality rather than to optimize prediction based on a single geometric metric. In addition, the thickness (5 mm) and volume (5 mL) thresholds were selected a priori to ensure procedural simplicity and operational consistency, rather than to define outcome-optimized cutoffs, and should therefore be interpreted as preliminary benchmarks for geometric assessment pending future data-driven refinement.

One-month imaging confirmed that adequate apical spread remains the Achilles' heel of hydrogel placement. In our cohort, apex volume ≥ 5 mL was achieved in only 45% of patients, and apex thickness ≥ 5 mm in 80%. Because the rectum meets the prostate apex obliquely, limited needle excursion and gravity-driven hydrogel redistribution likely contribute to this deficit. To address this challenge, we implemented a real-time saline hydrodissection protocol with immediate contour assessment to identify under-dissected regions, followed by targeted hydrogel injection biased toward deficient areas. This approach yielded more symmetric and reproducible rectoprostatic separation, particularly in the anatomically constrained apical region.

Several limitations merit consideration. First, the retrospective, single-institution design limits external generalizability, underscoring the need for prospective multi-center validation of the VS. Second, imaging was confined to one month after implantation, precluding assessment of long-term spacer stability and late toxicity; nonetheless, early morphology remains clinically relevant because more than 80% of the LDR seed dose is delivered within 3 months. Third, a minority of cases exhibited suboptimal VS despite technical refinement, likely reflecting fixed anatomic factors such as a narrow rectoprostatic angle or bulky seminal vesicles. Fourth, the VS is a cross-sectional metric derived from day 30 morphology and does not capture temporal changes in spacer configuration. Day 0 assessment was limited to non-contrast CT, on which the hydrogel spacer is radiolucent, preventing reliable volumetric or thickness measurements; therefore, temporal stability or reproducibility of spacer morphology could not be evaluated in this study. Accordingly, the clinical interpretation of the VS is intentionally confined to

https://doi.org/10.3857/roj.2025.00619

technical adequacy and procedural quality rather than long-term clinical outcome surrogacy. In addition, the incremental contribution of volumetric parameters beyond thickness alone was not formally evaluated in this initial analysis and should be addressed in future studies focusing on dose correlation and inter-observer reproducibility. Because this study was not designed to evaluate binary clinical endpoints or toxicity outcomes, data-driven cutoff determination using receiver operating characteristic analysis, toxicity correlation, or Youden index was not feasible. Accordingly, the selected thresholds should be regarded as preliminary operational benchmarks, and future studies will be required to refine them using outcome- or reproducibility-based validation frameworks. Finally, although MRI-based volume segmentation adds procedural complexity, volume captures longitudinal continuity and directional extent of the hydrogel column that cannot be inferred from point-based thickness measurements alone. The selected VS thresholds (5 mL for volume and 5 mm for thickness) were chosen a priori for procedural simplicity and should be regarded as preliminary rather than outcome-optimized benchmarks.

Future studies should prospectively validate the VS across institutions, incorporate serial imaging to characterize spacer resorption dynamics, and link score strata to late gastrointestinal toxicity, quality-of-life outcomes, and cost-effectiveness. Such efforts will refine patient selection, optimize insertion technique, and establish the VS as a benchmark for emerging spacer materials and delivery platforms.

In conclusion, meticulous technique—including apex-biased injection, intra-procedural symmetry checks, and structured operator feedback using the VS—is essential to maximize the rectal-sparing benefit of hydrogel spacers in LDR prostate brachytherapy while preserving target dosimetry. The VS offers a practical, morphology-based procedural quality-assurance framework that complements conventional dosimetric evaluation. Future prospective, multi-institutional studies incorporating serial imaging and longer follow-up are warranted to further refine this scoring system and to clarify how spacer morphology characterized by the VS relates to late gastrointestinal toxicity, patient-reported outcomes, and optimization of patient- and anatomy-specific insertion strategies.

Statement of Ethics

This retrospective study protocol was reviewed and approved by the Institutional Review Board of Severance Hospital (IRB approval no. 4-2025-0546) in accordance with the 1964 Declaration of Helsinki and its later amendments. Written informed consent was waived by the Institutional Review Board of Severance Hospital.

Conflict of Interest

No potential conflict of interest relevant to this article was reported.

Acknowledgments

We thank all medical staff in Yonsei Cancer Center for their support in patient care, and approval of introducing rectal hydrogel spacers for prostate cancer.

Funding

None.

Author Contributions

Conceptualization, HC, JC; Data collection and anonymization, HC, SJL, YP, WK, HL, JC; Statistical analysis, HC; Supervision, JC; Writing of the original draft, HC, JC; Writing of the review and editing, HC, JC; Approval of final manuscript: all authors.

Data Availability Statement

The data that support the findings of this study are not publicly available due to the information could compromise the privacy of research participants but are available from the corresponding author upon reasonable request.

Supplementary Materials

Supplementary materials can be found via https://doi.org/10.3857/roj.2025.00619.

References

1. Grimm P, Billiet I, Bostwick D, et al. Comparative analysis of prostate-specific antigen free survival outcomes for patients with low, intermediate and high risk prostate cancer treatment by radical therapy: results from the Prostate Cancer Results Study Group. BJU Int 2012;109 Suppl 1:22–9.
2. Mariados N, Sylvester J, Shah D, et al. Hydrogel spacer prospective multicenter randomized controlled pivotal trial: dosimetric and clinical effects of perirectal spacer application in men undergoing prostate image guided intensity modulated radiation therapy. Int J Radiat Oncol Biol Phys 2015;92:971–7.
3. Hamstra DA, Mariados N, Sylvester J, et al. Continued benefit to

rectal separation for prostate radiation therapy: final results of a phase III trial. Int J Radiat Oncol Biol Phys 2017;97:976–85.
4. Lin YH, Loon W, Tacey M, et al. Impact of hydrogel and hyaluronic acid rectal spacer on rectal dosimetry and toxicity in low-dose-rate prostate brachytherapy: a multi-institutional analysis of patients' outcomes. J Contemp Brachytherapy 2021;13:605–14.
5. Kubo K, Kenjo M, Kawabata H, et al. Hydrogel spacer shrinkage during external-beam radiation therapy following low-dose-rate brachytherapy for high-risk prostate cancer: a case series. J Med Case Rep 2021;15:296.
6. Brenneman RJ, Goddu SM, Andruska N, et al. Feasibility of same-day prostate fiducial markers, perirectal hydrogel spacer placement, and computed tomography and magnetic resonance imaging simulation for external beam radiation therapy for low-risk and intermediate-risk prostate cancer. Pract Radiat Oncol 2022;12:e117–22.
7. Polamraju P, Bagley AF, Williamson T, Zhu XR, Frank SJ. Hydrogel spacer reduces rectal dose during proton therapy for prostate cancer: a dosimetric analysis. Int J Part Ther 2019;5:23–31.
8. Hwang ME, Black PJ, Elliston CD, et al. A novel model to correlate hydrogel spacer placement, perirectal space creation, and rectum dosimetry in prostate stereotactic body radiotherapy. Radiat Oncol 2018;13:192.
9. Fischer-Valuck BW, Chundury A, Gay H, Bosch W, Michalski J. Hydrogel spacer distribution within the perirectal space in patients undergoing radiotherapy for prostate cancer: impact of spacer symmetry on rectal dose reduction and the clinical consequences of hydrogel infiltration into the rectal wall. Pract Radiat Oncol 2017;7:195–202.
10. Giacometti V, McLaughlin O, Comiskey P, et al. Validation of a quality metric score to assess the placement of hydrogel rectal spacer in patients treated with prostate stereotactic radiation therapy. Adv Radiat Oncol 2024;9:101396.
11. Meyer AR, Dharmaraj D, Harb R, Pavlovich CP, Allaf ME, Gorin MA. Perirectal hydrogel spacer placement prior to prostate radiation therapy using a probe-mounted needle guide. Clin Transl Radiat Oncol 2021;29:102–5.
12. Kobayashi H, Eriguchi T, Tanaka T, et al. An optimal method of hydrogel spacer insertion for stereotactic body radiation therapy of prostate cancer. Jpn J Radiol 2024;42:406–14.
13. Pinkawa M, Haddad H, Schlenter M, et al. Application of a radiopaque viscous hydrogel spacer for prostate cancer radiation therapy: a prospective phase 2 study. Pract Radiat Oncol 2024;14:57–64.
14. Icht O, Schlosser S, Weinstock-Sabbah M, et al. The role of a radiopaque peri-rectal hydrogel spacer in aiding accurate daily image-guidance for prostate stereotactic radiotherapy. Front Oncol 2024;14:1386058.
15. Gejerman G, Goldstein MM, Chao M, et al. Barrigel spacer injection technique. Pract Radiat Oncol 2024;14:e57–61.
16. Song D, Dabkowski M, Costa P, et al. Prospective, randomized controlled pivotal trial of biodegradable balloon rectal spacer for prostate radiation therapy. Int J Radiat Oncol Biol Phys 2024;120:1410–20.
17. Hama Y, Tate E. Quantitative evaluation of volume change of perirectal hydrogel spacer by Dixon-based water-only images. J Radiosurg SBRT 2022;8:105–8.

 https://doi.org/10.3857/roj.2025.00619